Journal of Physics: Conference Series **455** (2013) 012007 doi:10.1088/1742-6596/455/1/012007

(Anti-)matter and hyper-matter production at the LHC with ALICE

Nicole Martin[1,2] (for the ALICE Collaboration)

[1] ExtreMe Matter Institute EMMI and Research Division, GSI Helmholtzzentrum für Schwerionenforschung, Darmstadt, Germany
[2] Institut für Kernphysik, Technische Universität Darmstadt, Darmstadt, Germany

E-mail: n.martin@gsi.de

Abstract. ALICE is the experiment at the CERN LHC dedicated to the investigation of high energy nucleus–nucleus collisions. Its excellent particle identification capabilities allow for the measurement of rarely produced particles, like hypernuclei and light nuclei (and their anti-particles). We present here results from Pb–Pb collisions at a center of mass energy of $\sqrt{s_{\rm NN}}$ = 2.76 TeV per nucleon–nucleon pair. In particular the measurement of $^3\overline{\rm He}$ and $^4\overline{\rm He}$ is discussed. In addition the reconstruction of (anti-)hypertritons via their mesonic decay ($^3_\Lambda{\rm H} \rightarrow {}^3{\rm He} + \pi$) is presented. Searches for even lighter hypermatter states, i.e. $\Lambda\Lambda$ (also known as H-Dibaryon) and Λn bound states, are dicussed. The results are compared with thermal model predictions.

1. Introduction

The measurement of light (anti-)nuclei and (anti-)hypernuclei, created in heavy-ion collisions is challenging as the production probability decreases with increasing mass. The production yields of these particles can for example be predicted by thermal models based on an analysis of lighter particles [1, 2]. The chemical freeze-out temperature T, the volume V and the baryo-chemical potential μ_B are the only three parameters in this approach. If particle ratios instead of yields are calculated the volume cancels out and the yield ratios, as for example $\frac{^n\overline{\rm He}}{^n{\rm He}}$, scale with $\exp(-2n\mu_B/T)$. Therefore, the fit to the data of lighter particles provides constraints for the baryo-chemical potential μ_B and the chemical freeze-out temperature T. The production yields depend on the center-of-mass energies $\sqrt{s_{\rm NN}}$ of the colliding nuclei. Figure 1 shows thermal model predictions for particle ratios as a function of $\sqrt{s_{\rm NN}}$ together with experimental data from AGS, SPS and RHIC [1]. A fit to the experimental data at the highest energy available before the startup of the LHC, namely $\sqrt{s_{\rm NN}}$ = 200 GeV per nucleon–nucleon pair, gives: $\mu_B = 24 \pm 2$ MeV and T = 162 ± 2 MeV. The analysis can be extended by investigating also light nuclei and hypernuclei, which are discussed in section 4. The lightest anti-hypernucleus, the anti-hypertriton $^3_\Lambda\overline{\rm H}$ was first measured by the STAR Collaboration [3]. The experimental ratios measured by STAR can be compared with the theoretical predictions from a thermal model: the experimental ratios of $^3{\rm He}/^3\overline{\rm He}$ and $^3_\Lambda{\rm H}/^3_\Lambda\overline{\rm H}$ are in good agreement with the model predictions, but the measured ratios of $^3{\rm He}/^3_\Lambda{\rm H}$ and $^3\overline{\rm He}/^3_\Lambda\overline{\rm H}$ are about two standard deviations larger then the predicted ratios [1]. To further investigate this discrepancy, additional experimental data is needed. The energy reached in heavy-ion collisions at the LHC provide the opportunity to

measure such particles in unprecedented abundances. Up to now in two periods in the years 2010 and 2011, each roughly four weeks long, data from Pb–Pb collisions at $\sqrt{s_{\rm NN}} = 2.76\,\text{TeV}$ per nucleon–nucleon pair were recorded. The ALICE detector system [4] is well suited to measure the rarely produced states created in Pb–Pb collisions due to its unique particle identification capabilities. Exotic states like a possible Λn bound state or the H-Dibaryon are also investigated. The H-Dibaryon is a bound state of *uuddss* (ΛΛ) and was first predicted by Jaffe in a bag model calculation [5]. Recent lattice QCD calculations [6, 7] also suggest a bound state, with binding energies in the range 13-50 MeV/c. A chiral extrapolation of these lattice calculations to a physical pion mass resulted in a H-Dibaryon unbound by either 13 ± 14 MeV/c [8] or it is lies close to the Ξp threshold [9]. This renewed the interest in the experimental searches for the H-Dibaryon. The results related to these searches of such exotic bound states are presented in section 5.

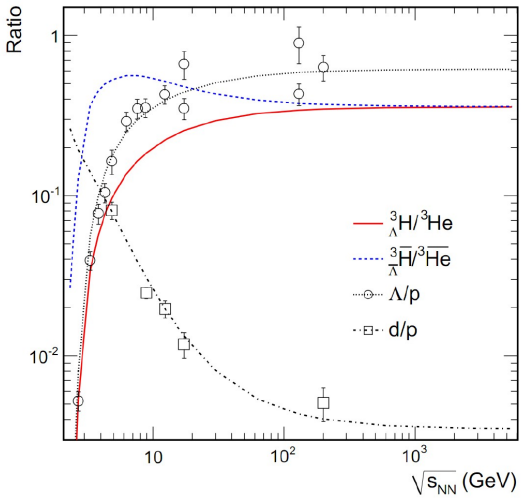

Figure 1. Thermal model predictions for particle ratios as a function of the center of mass energy per nucleon–nucleon pair ($\sqrt{s_{NN}}$) for central Pb–Pb collisions [1].

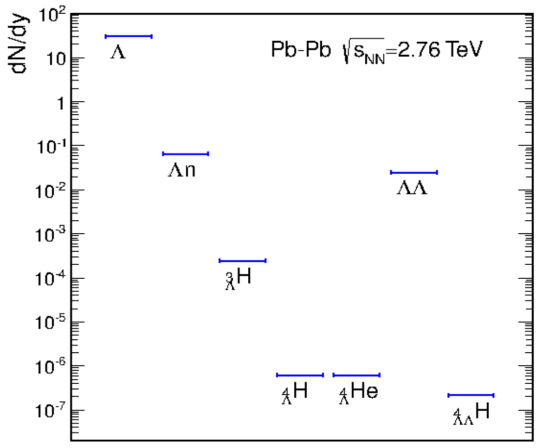

Figure 2. Shown here are predictions for the production yield dN/dy from thermal model calculations for various particles for central Pb–Pb collisions. [10].

2. The ALICE detector system

The ALICE detector is one of the four large experiments at the Large Hadron Collider (LHC) at the European Organization for Nuclear Research (CERN) in Geneva, Switzerland. Besides Pb–Pb collisions, proton-proton and p-Pb collisions are investigated. The ALICE detector is in total 26 meters long, 16 meters high and 16 meters wide. It weighs 10,000 tons and is located at the Interaction Point 2 of the LHC. It has a central barrel which holds most of the detector systems, a single arm backward muon spectrometer and two Zero Degree Calorimeters (ZDC) to distinguish between central and peripheral collisions. The four detectors in the central part, which all cover a pseudo-rapidity interval of $|\eta| \leq 0.9$ over the full azimuth, are the Inner Tracking System (ITS) and the Time Projection Chamber (TPC) for tracking, a Time Of Flight (TOF) detector for clear π/K and K/p separation at intermediate momenta and the Transition Radiation Detector (TRD) for electron identification. A schematic view of the ALICE detector is shown in figure 3.

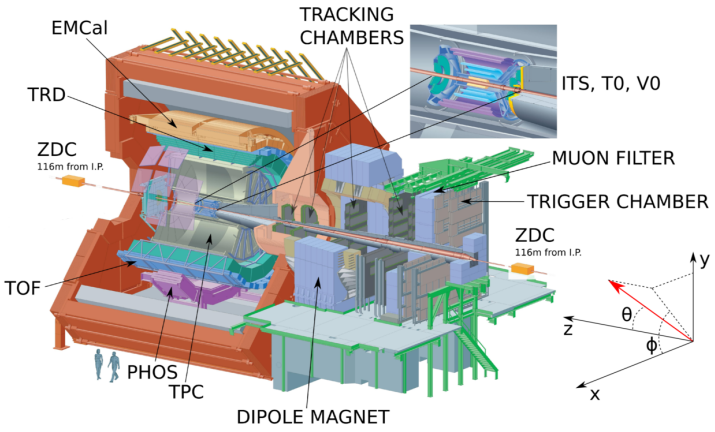

Figure 3. The ALICE detector system together with the ALICE coordinate system: right-handed orthogonal Cartesian system with the point of origin at the interaction point. The positive x,y,z-axes of the Cartesian coordinate system are shown together with the spherical coordinates r, ϕ and θ.

Particle identification
The precise particle identification (PID) and continous tracking from very low (100 MeV/c) to very high p_{T} (20 GeV/c) is a unique speciality of the ALICE detector. The PID used in the analysis described in this proceedings takes advantage of three different techniques: the specific energy loss (dE/dx), which is described by the Bethe-Bloch formula [11], measured with the TPC is used to identify particles in particular at low and high momenta (relativistic rise). This allows the identification of all particle species, from the lightest (electron) to the heaviest (anti-nuclei). The resolution of the TPC ranges from $\sigma \approx 5.2$ % in pp collisions to 6.5% (2010), respectively 7.2% (2011), in central Pb–Pb collisions. For intermediate p_{T} the TOF detector is used. The TOF measurement has a resolution of $\sigma \approx 85$ ps in Pb–Pb collisions and 120 ps in pp collisions. The TOF performance allows a 2σ p/K-separation up to a momentum of 5 GeV/c. Figure 4 shows the velocity β measured with the TOF detector as a function of the momentum p of the particle for Pb–Pb collisions. In addition unstable particles are identified via their decay topologies.

3. Anti-nuclei
Light anti-nuclei such as anti-protons $\overline{p}$, anti-deuterons $\overline{d}$, anti-tritons $\overline{t}$ and anti-helium $^3\overline{\mathrm{He}}$ are produced even in pp collisions in a significant amount. More nuclei than anti-nuclei are detected, but in principle the anti-baryon to baryon ratio at the LHC energies is close to unity thus also light nuclei and their corresponding anti-nuclei are expected to have similar yields. On the matter side a substantial background is created via knockout from the material, whereas anti-particles suffer only from annihilation when detector material is crossed. This is demonstrated in figures 5 and 6. They show the distance of closest approach (DCA) to the primary vertex in the xy-plane (DCA$_{XY}$) for different DCA in the z direction (DCA$_Z$). Whereas the number of deuterons increases with increasing DCA$_Z$, because of the deuterons which are knocked out from the detector material, the distributions for anti-deuteron stay the same. The knockout is a significant problem at low p_{T}. Therefore anti-matter studies benefit from a cleaner sample.

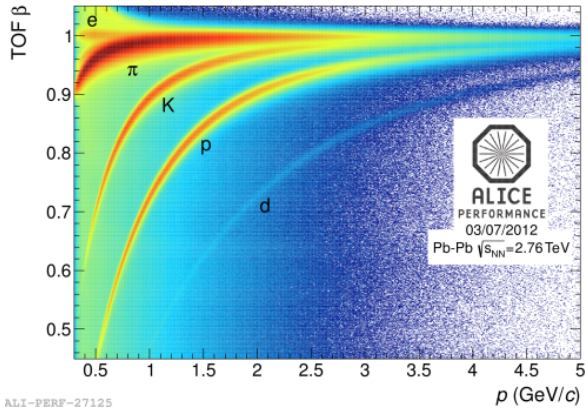

Figure 4. The velocity β measured with the TOF detector as function of the momentum p of the particle.

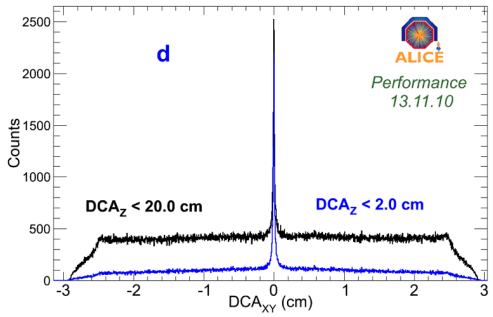

Figure 5. DCA_{XY} distribution for different DCA_Z values for deuterons.

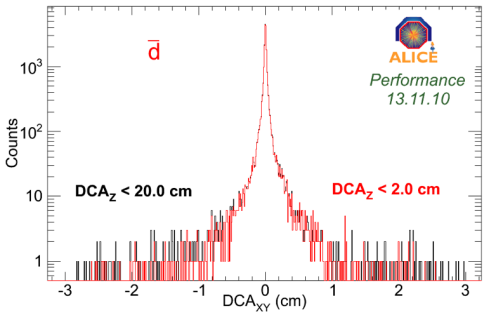

Figure 6. DCA_{XY} distribution for different DCA_Z values for anti-deuterons.

Anti-helium-4 $^4\overline{\mathrm{He}}$

For the identification of the $^4\overline{\mathrm{He}}$ we first selected all events, which had at least one particle with a $\mathrm{d}E/\mathrm{d}x$ corresponding to a $^3\overline{\mathrm{He}}$ or a higher mass. This offline "trigger" is indicated in figure 7 with a dashed line. Then we identified $^4\overline{\mathrm{He}}$ candidates in a 3σ range around the theoretical Bethe-Bloch curve. But this is not sufficient enough, especially at higher rigidity $\frac{p}{z}$ (the momentum p of the particle divided by its charge number z) where the two Bethe-Bloch curves of $^4\overline{\mathrm{He}}$ and $^3\overline{\mathrm{He}}$ are very similar. Therefore we use in addition the information from the TOF detector to calculate the $\frac{m^2}{z^2}$. The result is shown in the inlay in figure 7. The particles with the ratio of m^2 to z^2 which corresponds to $^4\overline{\mathrm{He}}$ are indicated with larger (red) markers in the $\mathrm{d}E/\mathrm{d}x$ vs. rigidity figure. We identified 10 $^4\overline{\mathrm{He}}$ using the TPC and TOF, corresponding to $23 \cdot 10^6$ events of a trigger mix (central, semi-central and minimum bias). The first $^4\overline{\mathrm{He}}$ nuclei were recently observed by the STAR Collaboration at RHIC [12].

4. (Anti-)Hypertriton

The investigation of hypernuclei has a long tradition in nuclear physics. They were discovered in the 1950s by M. Danysz and J. Pniewski in a photographic emulsion exposed to cosmic rays [13]. Hypernuclei are nuclei, in which at least one hyperon is bound in addition to the normal nucleons. All hyperons are unstable, even if they are bound in a nucleus. Nuclei of mass 5 only exist in the form of hypernuclei $\left({}^5_\Lambda\mathrm{He}\right)$. Therefore hypernuclei give access

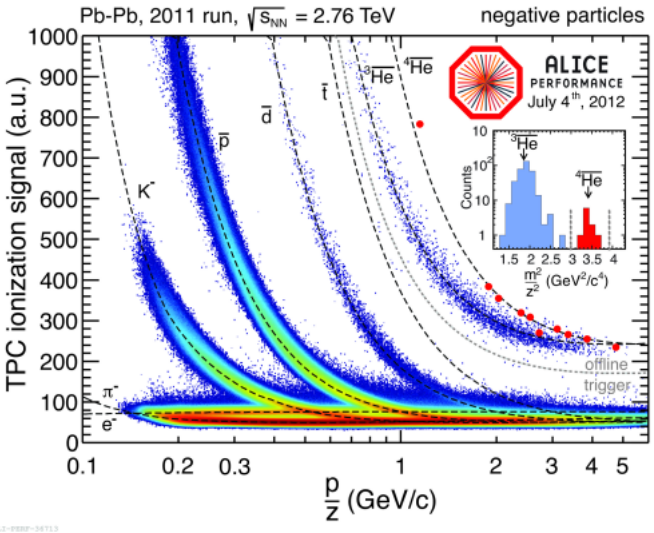

Figure 7. TPC $\mathrm{d}E/\mathrm{d}x$ spectrum for negative particles after a selection of events that contain at least one $^3\overline{\mathrm{He}}$ or $^4\overline{\mathrm{He}}$ candidate for the 2011 data. The inlet shows the $\frac{m^2}{z^2}$ distribution for this pre-selected data. The 10 $^4\overline{\mathrm{He}}$ nuclei clearly identified by TPC and TOF are indicated as red dots.

to the next higher mass (anti-)nucleus, which will be measurable in heavy-ion collisions. The (anti-)hypertriton has a mass of $2.991 \pm 0.001 \pm 0.002\,\mathrm{GeV}/c^2$ and a decay length of $c\tau = 5.5^{+2.7}_{-1.4} \pm 0.8$ cm [3]. This is a similar decay length as the one of the free Λ particle ($c\tau \approx 7.8\,\mathrm{cm}$). We identify the (anti-)hypertriton candidates via their decay daughters $\left(\pi, ^3\mathrm{He}\right)$. We first look for light nuclei $\left(^3\mathrm{He}, ^3\overline{\mathrm{He}}\right)$ which are daughter tracks originating from decay vertices. They are identified via the TPC $\mathrm{d}E/\mathrm{d}x$ information. If the second daughter is identified as a pion, we reconstruct the invariant mass of the pair. The resulting invariant mass distributions for the Pb–Pb data corresponding to $23 \cdot 10^6$ events of a trigger mix (central, semi-central and minimum bias) are shown in figure 8 and figure 9. The signal of the (anti-)hypertriton has a mean mass of $2.990 \pm 0.001\,\mathrm{GeV}/c^2$ $\left(2.993 \pm 0.001\,\mathrm{GeV}/c^2\right)$ and a width of $3.35 \pm 0.7\,\mathrm{MeV}/c^2$ $\left(2.0 \pm 1.2\,\mathrm{MeV}/c^2\right)$.

5. Exotic bound states

We investigate two possible bound states: the Λn bound state and the H-Dibaryon ($\Lambda\Lambda$).

Λn bound state

We search for a possible Λn bound state, which decays into a deuteron and a pion, in the data set of Pb–Pb collisions from 2010 ($13.8 \cdot 10^6$ min. bias events). The HypHI experiment at GSI observes a signal, compared to mixed events, in the $d + \pi^-$ which they connect to the possible existence of a new bound state [14]. We investigate here only the $\overline{\Lambda \mathrm{n}}$ bound state, because of the lower background compared to the corresponding particle. To estimate the efficiency for the detection of the $\overline{\Lambda \mathrm{n}}$ Monte Carlo sample has been produced, where the $\overline{\Lambda \mathrm{n}}$ was generated flat in rapidity y and in transverse momentum p_T. We assume the lifetime to be that of the Λ particle. As we do not know the true shape of the p_T spectrum we estimate it from the extrapolation of blast-wave fits for π, K, p done at the same energy. Blast-wave functions describe the shape of p_T spectra in heavy-ion collisions quite well, since the blast-wave describes the thermal part and the radial flow visible in these spectra. The resulting blast-wave is normalised to unity

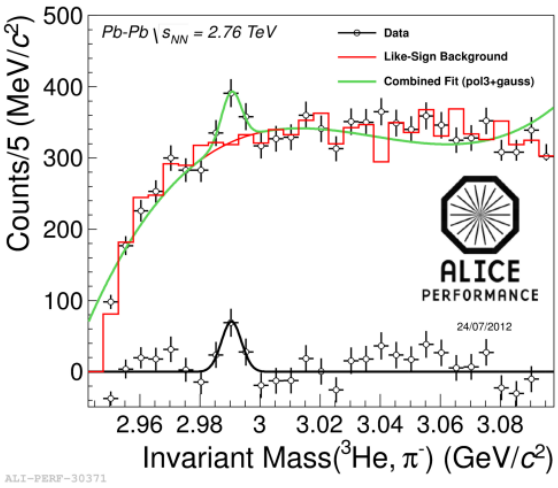

Figure 8. Invariant mass distribution of $^3\mathrm{He} + \pi^-$.

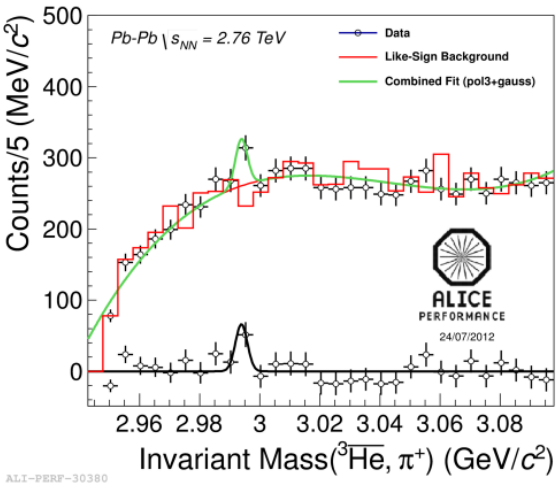

Figure 9. Invariant mass distribution of $^3\overline{\mathrm{He}} + \pi^+$.

and convoluted with the correction factor (efficiency × acceptance) to get a weighted efficiency. The unknown p_T shape is the main source of uncertainty. therefore, we use different functions for the systematics (limiting cases: blast-wave of deuteron and ^{3}He). To estimate the number of $\overline{\Lambda\mathrm{n}}$ particles, which we expect to measure, we need in addition also the branching ratio and the yield $\mathrm{d}N/\mathrm{d}y$. The branching ratio depends on the binding energy shown in figure 10. The production yield $\mathrm{d}N/\mathrm{d}y$ is taken from thermal model predictions, see figure 2. The resulting number of $\overline{\Lambda\mathrm{n}}$ particles which we expect is $N_{\overline{\Lambda\mathrm{n}},rec} = N_{events} \cdot Acc \times Eff \cdot BR \cdot \frac{\mathrm{d}N}{\mathrm{d}y} \cdot \mathrm{d}y \approx 4000$. For the data analysis we follow a similar strategy as for the hypertriton. We search for displaced decay vertices. If we can identifiy one of the daughter tracks as a deuteron and the second daughter as a pion, we calculate the invariant mass of these candidates. The result is shown in figure 12 (black points) together with the systematic error (grey band) and the peak which we expect from the Monte Carlo estimation and its corresponding error. So far we have no visible signal. From this non observation we can set an upper limit: $\mathrm{d}N/\mathrm{d}y \leq 1.5 \cdot 10^{-3}\,(99\,\%CL)$. This is a factor of 10 different to the thermal model input $\mathrm{d}N/\mathrm{d}y = 1.65 \cdot 10^{-2}$. However, the model describes the yields of the lighter hadrons and the hypertriton measured by STAR at $\sqrt{s_{NN}} = 200$ GeV correctly within uncertainties.

H-Dibaryon ($\Lambda\Lambda$)
For the H-Dibaryon we investigate two possible cases. In the first case the mass of the H-Dibaryon m_H is below the $\Lambda\Lambda$ threshold, such that the H-Dibaryon would be weakly bound and a measurable decay channel would be $\mathrm{H} \to \Lambda + p + \pi$. The mass of the H-Dibaryon would then lie between $2.2\,\mathrm{GeV}/c^2 < m_\mathrm{H} < 2.231\,\mathrm{GeV}/c^2$. In the second case the mass of the H-Dibaryon m_H is above the $\Lambda\Lambda$ threshold, such that the H-Dibaryon would be a resonant state and a measurable decay channel would be $\mathrm{H} \to \Lambda + \Lambda$. The mass of the H-Dibaryon would then lie above $m_\mathrm{H} > 2.231\,\mathrm{GeV}/c^2$. The analysis strategy for the H-Dibaryon is very similar as for the $\overline{\Lambda\mathrm{n}}$ bound state described above, except that here a second V0 type decay particle is involved. The result is shown in figure 13. Again we want to estimate the number of H-Dibaryons, which we expect from the current statistics from the Pb–Pb run of 2010 ($13.8 \cdot 10^6$ min. bias events). Therefore, we needed again estimates of the branching ratio and the yield $\mathrm{d}N/\mathrm{d}y$. The branching ratio as function of the binding energy is shown in figure 11. The production yield $\mathrm{d}N/\mathrm{d}y$ is

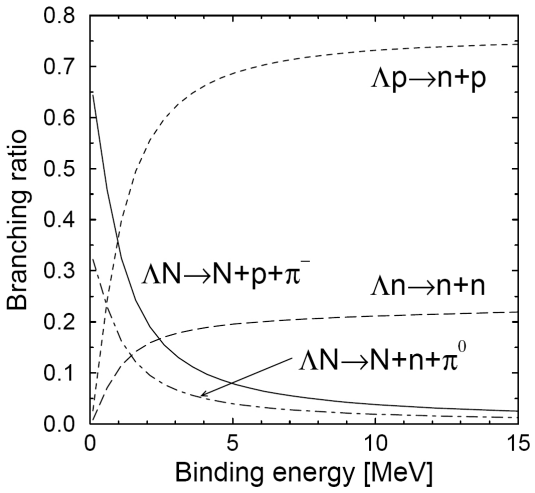

Figure 10. Theory predictions for the branching ratios for different decay channels of the Λn and the Λp [15].

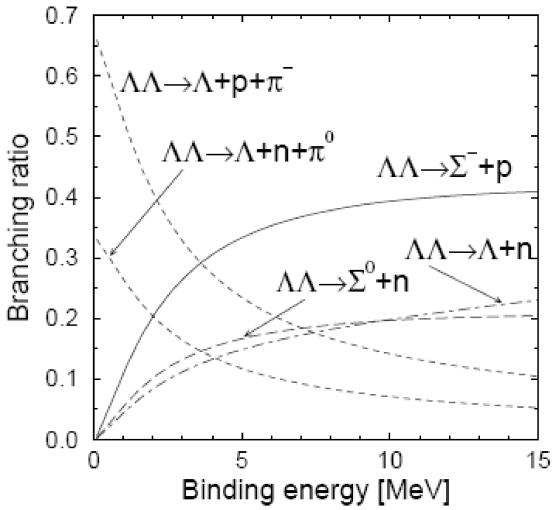

Figure 11. Theory predictions for the branching ratios for different decay channels of the H-Dibaryon [16].

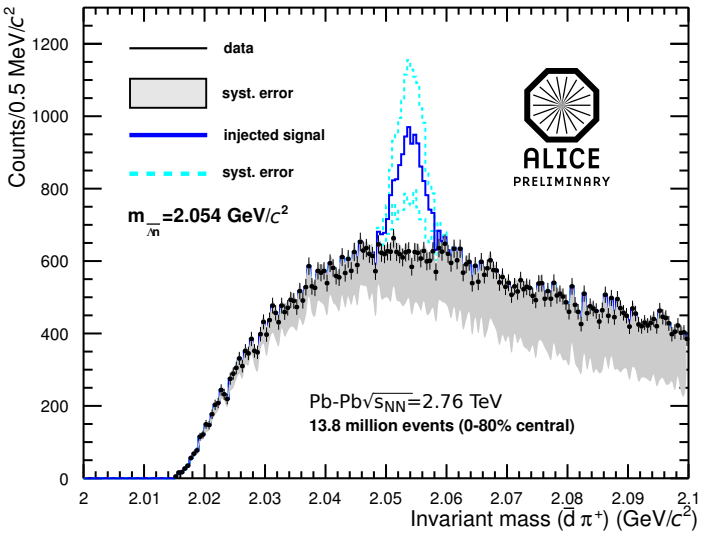

Figure 12. Invariant mass distribution for $d + \pi^+$. The figure also show the expected signal for the $\overline{\Lambda n}$ bound state.

again taken from the thermal model predictions, see figure 2. This results in 211 strongly bound H-Dibaryons which we should detect and 1350 lightly bound particles. The invariant mass distribution for the data is shown in figure 13 together with the two peaks, which we obtained from the Monte Carlo simulations. Again we see no hint of a signal from the data. From the non observation we can again obtain upper limits. For a strongly bound H we can set it to $\mathrm{d}N/\mathrm{d}y \leq 8.4 \cdot 10^{-4}\,(99\,\%CL)$ and for a lightly bound H $\mathrm{d}N/\mathrm{d}y \leq 2 \cdot 10^{-4}\,(99\,\%CL)$. Compared to the thermal model prediction $\mathrm{d}N/\mathrm{d}y = 3.1 \cdot 10^{-3}$ a discrepancy of a factor 10 is observed.

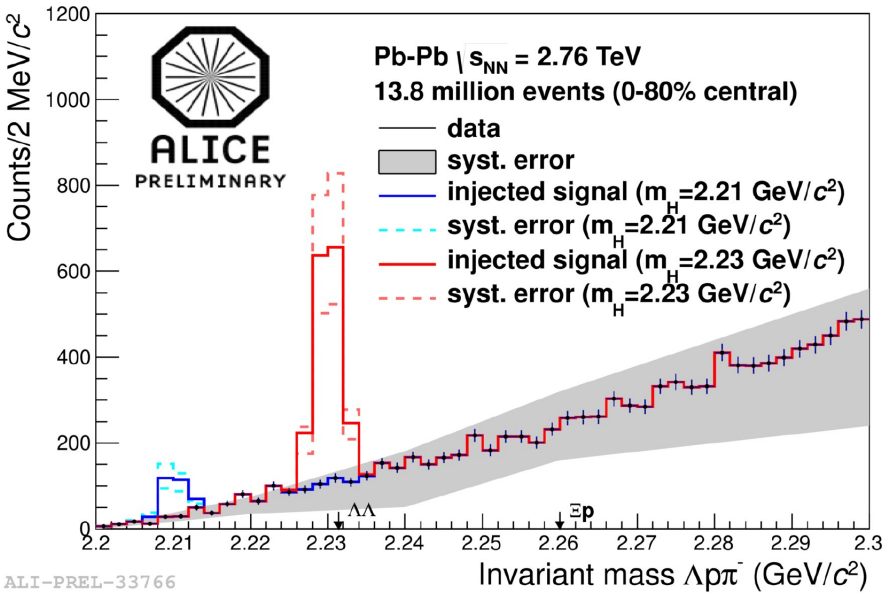

Figure 13. Invariant mass distribution for $\Lambda + p + \pi^-$. The figure also shows the expected signal for the two possible H-Dibaryons, which we investigated.

6. Summary and Outlook

We have shown that by combining the different particle identification techniques, e.g. TPC $\mathrm{d}E/\mathrm{d}x$ and TOF, the ALICE detector is well suited for the detection of stable, weakly and strongly decaying particle species up to high masses. We have observed 10 $^4\overline{\mathrm{He}}$ nuclei. The (anti-)hypertriton signal has also been observed and the work on the p_T spectra and the measurement of the lifetime is ongoing. Upper limits for the $\overline{\Lambda\mathrm{n}}$ bound state and for two bound cases for the H-Dibaryon were obtained. Final conclusion on the existence of these exotic particles will be possible with larger statistics, as planned within the ALICE upgrade studies.

References

[1] Andronic A, Braun-Munzinger P, Stachel J and Stöcker H 2011 *Phys. Lett.* B **697** 203
[2] Cleymans J, Kabana S, Kraus I, Oeschler H, Redlich K and Sharma N 2011*Phys. Rev.* C **84** 054916
[3] Abelev B I *et al* (STAR Collaboration) 2010 *Science* **328** 58
[4] Aamodt K *et al* (ALICE Collaboration) 2008 *JINST* **3** S08002
[5] Jaffe R 1977 *Phys. Rev. Lett.* **38** 195 and erratum ibid 1977 **38** 617
[6] Inoue T, Ishii N, Aoki S, Doi T, Hatsuda T, Ikeda Y, Murano K, Nemura H and Sasaki K (HAL QCD Collaboration) 2011 *Phys. Rev. Lett.* **106** 162001
[7] Beane S R *et al* (NPLQCD Collaboration) 2011 *Phys. Rev. Lett.* **106** 162002
[8] Shanahan P E, Thomas A W and Young R D 2011 *Phys. Rev. Lett.* **107** 092004
[9] Haidenbauer J and Meißner U-G 2011 *Phys. Lett.* B **706** 100
[10] Andronic A private communication
[11] Bethe H 1930 *Annalen der Physik* **397** 325
[12] Agakishiev H *et al* (STAR Collaboration) 2011 *Nature* **473** 353
[13] Danysz M and Pniewski J 1953 *Bull. Acad. Pol. Sci.* III **1** 42;
Danysz M and Pniewski J 1953 *Phil. Mag.* **44** 348
[14] http://www.bnl.gov/hhi/files/talks/TakehikoSaito.pdf, as shown 1.3.2012 at the Riken-BNL workshop on "Hyperon-Hyperon Interactions and Searches for Exotic Di-Hyperons in Nuclear Collisions"
[15] Schaffner-Bielich J private communication
[16] Schaffner-Bielich J, Mattiello R and Sorge H 2000 *Phys. Rev. Lett.* **84** 4305